Odorant receptor orthologues in conifer-feeding beetles display conserved responses to ecologically relevant odors

Short title: Conserved responses in odorant receptors

Rebecca E. Roberts[1], Twinkle Biswas[1], Jothi Kumar Yuvaraj[1], Ewald Grosse-Wilde[2,3], Daniel Powell[1,4], Bill S. Hansson[2], Christer Löfstedt[1], Martin N. Andersson[1*]

[1] Department of Biology, Lund University, Lund, Sweden

[2] Department of Evolutionary Neuroethology, Max Planck Institute for Chemical Ecology, Jena, Germany

[3] Present address: Faculty of Forestry and Wood Sciences, Czech University of Life Sciences Prague, Czech Republic

[4] Present address: Global Change Ecology Research Group, School of Science, Technology and Engineering, University of the Sunshine Coast, Sippy Downs, QLD, Australia

*** Correspondence:**

Martin N. Andersson, Department of Biology, Sölvegatan 37, SE-223 62 Lund, Sweden.

Email: martin_n.andersson@biol.lu.se

Phone: +46-(0)462229344

Keywords

Functional characterization; de-orphanization; HEK293 cells; evolutionary conservation; *Ips typographus*, *Dendroctonus ponderosae*; *Hylobius abietis*; Curculionidae.

Abstract

Insects are able to detect a plethora of olfactory cues in the environment using a divergent family of odorant receptors (ORs). Despite the divergent nature of this family, related species frequently express several evolutionarily conserved OR orthologues. In Coleoptera, it remains unknown whether OR orthologues have conserved or divergent functions in different species. We addressed this question through functional characterization of two groups of OR orthologues in three species of the Curculionidae (weevil) family, the conifer-feeding bark beetles *Ips typographus* ('Ityp') and *Dendroctonus ponderosae* ('Dpon') (both in subfamily Scolytinae), and the pine weevil *Hylobius abietis* ('Habi'; Molytinae). The ORs of *H. abietis* were annotated from antennal transcriptomes. Results show highly conserved response specificities, with one group of orthologues (HabiOR3/DponOR8/ItypOR6) responding exclusively to 2-phenylethanol (2-PE), and the other group (HabiOR4/DponOR9/ItypOR5) responding to angiosperm green leaf volatile (GLV) alcohols. Both groups of orthologues belong to the major coleopteran OR group 2B, and share a common ancestor with OR5 in the cerambycid *Megacyllene caryae*, also tuned to 2-PE, suggesting a shared evolutionary history of 2-PE receptors across two beetle superfamilies. The detected compounds are ecologically relevant for conifer-feeding curculionids, and are probably linked to fitness, with GLVs being used to avoid angiosperm non-host plants, and 2-PE being important for intraspecific communication and/or playing a putative role in beetle-microbe symbioses. To our knowledge, this study is the first to reveal evolutionary conservation of OR functions across several beetle species and hence sheds new light on the functional evolution of beetle ORs.

Introduction

Insects are able to detect thousands of different chemical cues that convey important information about the environment, including plant volatiles, microbial odors, and pheromones (Dahanukar, et al. 2005; Hansson and Stensmyr 2011; Stensmyr, et al. 2012; Kandasamy, et al. 2019). This sophisticated discernment of odors is possible via large suites of odorant receptors (ORs), which bind and detect odor molecules in peripheral olfactory sensory neurons (OSNs), triggering neuronal signals to be processed by the central nervous system (Clyne, et al. 1999; Vosshall, et al. 1999; Sato, et al. 2008; Wicher, et al. 2008; Brand, et al. 2018). These seven-transmembrane proteins form heteromeric complexes with a highly conserved co-receptor (Orco), which is necessary for odor responses in most insects by

contributing to the formation of a ligand-gated ion channel (Larsson, et al. 2004; Butterwick, et al. 2018).

The OR gene family evolves according to a birth-and-death model, in which duplication events represent the birth of genes, and deletion or pseudogenization their death (Nei, et al. 2008). Accordingly, OR genes are often found in tandem arrays on insect chromosomes, with significant variation in the size of OR repertoires between species (Andersson, et al. 2015; Benton 2015; Brand and Ramírez 2017). Frequently, the majority of ORs in a given species are present within species- or taxon-specific phylogenetic OR-lineage radiations (Mitchell, et al. 2020). Within such radiations, novel olfactory functions may evolve due to relaxed constraints or positive selection post gene duplication, provided the duplicated gene is retained and expressed (Andersson, et al. 2015; Hou, et al. 2021). Despite the general divergent nature of this receptor family, certain ORs are conserved across species, with simple (1:1) orthologous OR-pairs typically being present among related species. However, such clear orthology is usually rare or absent when comparing more distantly related insect species from different families, which has been shown in e.g., beetles (Coleoptera) (Mitchell and Andersson 2020; Mitchell, et al. 2020). Whether OR orthologues share the same or similar olfactory functions, or if functions have diverged in different species, has been studied primarily in moths (Lepidoptera) and mosquitos (Diptera). Such studies are important for advancing our understanding of the functional evolution of the insect OR family, as they may inform shared ecological relevance of certain compounds in different species, hence shared selection pressures acting on the olfactory sense of insects. For example, the host- and oviposition cues 1-octen-3-ol, indole and skatole, respectively, are detected by orthologous groups of ORs across several mosquito species (Dekel, et al. 2016; Ruel, et al. 2019). In moths, some olfactory functions are widely conserved among OR orthologues, including both the detection of specific plant odors and sex pheromone compounds, whereas other orthologues are functionally different (Gonzalez, et al. 2015; Guo, Huang, et al. 2021; Guo, Du, et al. 2021).

In contrast, nothing is known about the functions of OR orthologues in beetles, which is not surprising given the very few ORs that have been functionally characterized in this large order. The response profiles of seven ORs have been characterized from the Eurasian spruce bark beetle *Ips typographus* (‘Ityp’; Curculionidae) (Hou, et al. 2021; Roberts, et al. 2021; Yuvaraj, et al. 2021), two ORs from the red palm weevil *Rhynchophorus ferrugineus*

92 (Curculionidae) (Antony, et al. 2021; Ji, et al. 2021), one OR from the dark black chafer
93 *Holotrichia parallela* (Scarabaeidae) (Wang, et al. 2020), one OR from the Adonis ladybird
94 *Hippodamia variegata* (Coccinellidae) (Xie, et al. 2022) and three ORs from the hickory
95 borer *Megacyllene caryae* ('Mcar'; Cerambycidae) (Mitchell, et al. 2012). Among the
96 characterized ORs of this cerambycid, McarOR5 responded strongly to the male-produced
97 pheromone component 2-phenylethanol (2-PE) (Mitchell, et al. 2012). McarOR5 belongs to
98 the beetle OR subfamily named Group 2B, which contains conserved OR lineages with
99 receptors from several beetle families, including the large family of true weevils,
100 Curculionidae (Mitchell, et al. 2020). This beetle family harbors the damaging conifer-feeding
101 bark beetles of the Scolytinae subfamily and many other weevils that are pests of agriculture
102 and forestry, such as the pine weevil *Hylobius abietis* ('Habi'; Molytinae) (Shin, et al. 2018).
103 The 2-PE is ecologically relevant for several conifer-feeding beetles. For instance, it is part of
104 the attractive odor bouquets released by the fungal symbionts of *I. typographus* (Kandasamy,
105 et al. 2019) and the compound has also been identified from the hindgut of male beetles,
106 where it may be produced by yeasts (Leufvén, et al. 1984), in highest amounts before the
107 acceptance of females (Birgersson, et al. 1984). The compound is the primary odorant for one
108 of the characterized OSN classes of *I. typographus*, suggesting that this species is likely to
109 have an OR tuned to this compound. Also *Dendroctonus* bark beetles produce this compound
110 (Sullivan 2005), including the mountain pine beetle *D. ponderosae* ('Dpon'; Curculionidae),
111 in which 2-PE reduces the attraction to the aggregation pheromone (Pureswaran, et al. 2000).
112 In the pine weevil *H. abietis*, 2-PE operates as a strong anti-feedant present in deterrent non-
113 host plants (Eriksson, et al. 2008). Interestingly, 2-PE is also produced by gut bacteria of *H.*
114 *abietis*, and the behavior of this species, to cover their laid eggs with feces and frass
115 containing deterrent compounds, may protect the eggs from being eaten by conspecifics
116 (Borg-Karlson, et al. 2006; Axelsson, et al. 2017).
117
118 Due to the widespread use of 2-PE in the ecologies of conifer-feeding curculionids, we
119 hypothesized that the compound may be detected by evolutionarily and functionally
120 conserved ORs and that these receptors may be related to McarOR5. To test this hypothesis,
121 we used HEK293 cells to functionally characterize two clades with simple OR orthologues
122 from three curculionids (*I. typographus*, *D. ponderosae*, and *H. abietis*), i.e., the orthologues
123 in Group 2B that are positioned closest to McarOR5 in the OR phylogeny. The OR repertoires
124 of the two bark beetles have been previously reported (Andersson, et al. 2013; Andersson, et
125 al. 2019; Yuvaraj, et al. 2021); however, to obtain the OR sequences from *H. abietis* we

126 sequenced, analyzed, and annotated male and female antennal transcriptomes. Our results
127 show that 2-PE is indeed detected by functionally conserved and highly specific OR
128 orthologues in all three curculionids. These ORs share a common ancestor with McarOR5
129 suggesting functional conservation also across two beetle superfamilies (Curculionoidea and
130 Chrysomeloidea). Additionally, green leaf volatile (GLV) alcohols, abundant in non-host
131 angiosperm plants and generally avoided by conifer-feeding beetles (Zhang and Schlyter
132 2004), were detected by the second assayed clade of curculionid ORs. These receptors share
133 evolutionary history with the ORs detecting 2-PE. Altogether, our findings suggest strong
134 functional conservation in ORs detecting ecologically important odors, and thereby expand
135 our knowledge of the functional evolution of the OR family in the largest order of insects.
136

137 # Results

138 ***HabiOR annotation, expression, and phylogenetic analysis of ORs***

139 The HabiOrco gene and 78 HabiOR genes were annotated from the antennal transcriptome
140 assembly, of which 51 transcripts encoded full length proteins. The 28 partial HabiORs
141 encompassed 174 to 397 amino acids. Three of the ORs were extended by joining overlapping
142 sequences from two different transcripts. Annotation details and sequences of the HabiORs
143 are presented in Supplementary Table 1. Sequence reads from the male and female samples
144 were mapped to the open reading frames (ORFs) of annotated OR genes for estimation of
145 relative OR gene expression levels. This analysis showed that the HabiOrco gene is clearly
146 more highly expressed than any of the 78 HabiORs (Supplementary Table 1). The ORs
147 showed a range of expression levels (from 0.03% to 4.2% of the Orco expression in males;
148 from 0% to 5.7% in females), with no specific OR standing out as being particularly highly
149 expressed compared to the others. Expression was similar in the two sexes; the only putative
150 exceptions being the partial HabiOR27NC and HabiOR46NC that showed twice the
151 expression in females compared to males, and HabiOR48 with twice the expression in males
152 compared to females. Expression levels of the functionally characterized HabiOR3 and
153 HabiOR4 were intermediate, with a somewhat higher estimate for HabiOR4 in both sexes.
154

155 Recently, a phylogenetic analysis of the ORs across several coleopteran superfamilies defined
156 and revised nine main monophyletic groups of ORs (Mitchell, et al. 2020). Our phylogenetic
157 analysis including ORs from the Curculionidae and Cerambycidae shows that the distribution
158 of HabiORs among the nine OR groups is similar to that of the other two curculionids (*I.*

159 *typographus* and *D. ponderosae*) in the analysis (Figure 1), with most (55) ORs located within
160 Group 7, followed by Group 1 (9 ORs), Group 5A and 2A (5 ORs in each), and 2B (4 ORs).
161 The main differences between *H. abietis* and the two bark beetle species are the stronger bias
162 of HabiORs towards Group 7, including a large HabiOR-radiation of 26 receptors
163 (HabiOR23-HabiOR48), and comparatively few HabiORs in Group 5A. The latter may be
164 explained by the generally poor antennal expression of Group 5A ORs (Yuvaraj, et al. 2021);
165 indeed, the vast majority of Group 5A ORs from *D. ponderosae* was not found in the initial
166 transcriptome analyses (Andersson, et al. 2013), but later recovered from the genome
167 (Andersson, et al. 2019). As with other curculionids, our analysis indicates that *H. abietis*
168 entirely lacks ORs from Groups 3, 4, 5B, and 6. Similar to our previous study, the OR
169 phylogeny did not recapitulate the monophyly of Group 2B, which is likely explained by the
170 few species and narrow taxonomic range sampled in this study (Yuvaraj, et al. 2021).
171
172 Our OR phylogeny suggests 12 highly supported clades of simple (1:1:1) OR orthologues
173 conserved across the three curculionids (Figure 1). We also found that two of the McarORs
174 appear to have representative orthologues in at least some curculionids, i.e., McarOR2
175 grouped together with HabiOR1 and ItypOR11, and McarOR4 with DponOR6NTE and
176 ItypOR51 (Figure 1). Within OR Group 2B, two orthologous groups of curculionid ORs
177 (ItypOR5/DponOR9/HabiOR4 and ItypOR6/DponOR8/HabiOR3) were positioned close to
178 McarOR5, responding to 2-PE –a pheromone component in this species (Figure 1). Hence,
179 these six ORs were targeted for functional characterization to investigate whether
180 evolutionarily related beetle ORs within and between coleopteran superfamilies may have the
181 same response specificities. The amino acid identities between ItypOR5, DponOR9, HabiOR4
182 range from 50.5% to 57.8%, and for ItypOR6, DponOR8, and HabiOR3 between 60.0% and
183 67.5%.
184
185 ***Conserved responses to green leaf volatiles and 2-phenylethanol in OR orthologues***
186 The HEK cells transfected with each of the six above-mentioned beetle OR genes were
187 analyzed for OR protein detection using Western blots. Except for HabiOR4, the OR proteins
188 were clearly detected, and only from cells induced to express the exogenous receptor genes,
189 demonstrating proper regulation by the repressor system (Supplementary Figure 1). Gene
190 sequences codon-optimized for expression in human cells were used for the DponORs
191 because we had no access to biological material from this species (Roberts, et al. 2021).
192 Additionally, because the HabiOR4 protein was not detected from cell lines transfected with

193 the wildtype OR gene, this gene was also codon-optimized and used in functional assays. The
194 superscript HsCO (*Homo sapiens* Codon Optimized) was added to the names of codon
195 optimized OR genes.
196
197 In the OR phylogeny, the orthologous curculionid ORs HabiOR4, ItypOR5, and DponOR9
198 group most closely to the 2-PE receptor in the cerambycid *M. caryae* (McarOR5; Figure 1).
199 Screening experiments testing 62 ecologically relevant compounds at 30 µM concentration
200 showed that neither of these curculionid ORs responded to 2-PE. Instead, HabiOR4^{HsCO}
201 responded to five six-carbon green leaf volatile (GLV) alcohols, abundant in angiosperm non-
202 host plants, with significantly stronger responses in induced *vs.* non-induced cells (Figure
203 2A). *Z*3-hexenol elicited the strongest response in the screening experiments (7.3% increased
204 fluorescence; $F_{1,14} = 183.8$; $p < 0.001$), followed by slightly weaker and similar responses to
205 each of *E*2-hexenol, *Z*2-hexenol, and 1-hexanol (5.2-5.7%; $F_{1,14} = 48.9$-118.8; all $p < 0.001$),
206 and a yet weaker response to *E*3-hexenol (3.6%; $F_{1,14} = 40.5$; $p < 0.001$). Subsequent dose-
207 response experiments largely recapitulated the screening data in terms of response magnitudes
208 elicited by the five compounds at the higher concentrations (Figure 2B). Nevertheless, these
209 experiments indicated similar sensitivities to the four most active ligands (EC_{50} values: *Z*3-
210 hexenol – 7.99 µM, *E*2-hexenol – 3.88 µM, 1-hexanol – 2.85 µM, and *Z*2-hexenol – 7.34
211 µM), whereas the sensitivity to *E*3-hexenol was lower as shown by its weaker response at
212 most tested concentrations and the non-sigmoid shape of the dose-response curve (EC_{50} could
213 not be estimated).
214
215 A similar response profile was apparent for DponOR9^{HsCO} (Figure 2C). Again, *Z*3-hexenol
216 elicited the highest response in the screening experiments (4.5%; $F_{1,14} = 51.5$; $p < 0.001$),
217 followed by *E*2-hexenol (3.2%; $F_{1,14} = 44.2$; $p < 0.001$), *Z*2-hexenol (2.3%; $F_{1,14} = 48.3$; $p <$
218 0.001), and 1-hexanol (2.0%; $F_{1,14} = 24.6$; $p < 0.001$). The slightly increased fluorescence seen
219 upon stimulation with *E*3-hexenol was not statistically significant after correction for multiple
220 statistical comparisons. In contrast to HabiOR4, (+)-*trans*-4-thujanol elicited a significant
221 response in DponOR9^{HsCO} (3.5%; $F_{1,14} = 17.0$; $p = 0.001$); however, half of this response was
222 also evident in the non-induced control cells suggesting that factors unrelated to the DponOR
223 contributed to the cells' response. The two GLV compounds eliciting responses above 3%
224 increased fluorescence in the screening were further examined in dose-response trials,
225 showing somewhat stronger responses to *Z*3-hexenol as compared to *E*2-hexenol at the higher

226 concentrations but similar responses at intermediate and lower concentrations (Figure 2D).
227 EC_{50} values could not be estimated due to the shape of the dose-response curves.
228
229 ItypOR5 responded to the same four GLV alcohols as did DponOR9^{HsCO}, albeit with overall
230 lower response magnitudes (Figure 2E), which is in accordance with this OR being detected
231 as a fainter band on Western blot (Supplementary Figure 1) compared to the other orthologues
232 (see also Roberts, et al. 2021). The rank order between compounds was slightly different, with
233 *E*2-hexenol eliciting the highest response (3.3%; $F_{1,24} = 39.8$; $p < 0.001$), followed by *Z*2-
234 hexenol (2.2%; $F_{1,23} = 19.3$; $p < 0.001$), and similar responses to *Z*3-hexenol (1.6%; $F_{1,24} =$
235 27.9; $p < 0.001$) and 1-hexanol (1.6%; $F_{1,24} = 30.5$; $p < 0.001$). As with DponOR9^{HsCO}, the
236 slightly increased fluorescence elicited by *E*3-hexenol in induced cells was not statistically
237 significant after correction for multiple comparisons. *E*2-hexenol activated ItypOR5 in a dose-
238 dependent manner (Figure 2F; EC_{50} could not be estimated due to the shape of the dose-
239 response curve); the other GLVs were not assayed in dose-response experiments due to their
240 screening responses being below 3%.
241
242 Compared to the GLV-responding ORs, the orthologous receptors HabiOR3, ItypOR6, and
243 DponOR8 are positioned a bit further away from McarOR5 in the OR phylogeny; yet they are
244 part of the same OR clade (Figure 1). The three ORs all responded exclusively to 2-PE, with
245 significantly stronger responses in induced compared to non-induced cells. The highest
246 response was recorded for HabiOR3 (10.5% increased fluorescence; $F_{1,19} = 324.7$; $p < 0.001$;
247 Figure 3A), followed by ItypOR6 (5.7%; $F_{1,14} = 85.9$; $p < 0.001$; Figure 3E), and
248 DponOR8^{HsCO} (4.0%; $F_{1,14} = 80.4$; $p < 0.001$; Figure 3C). Each of these receptors responded
249 to 2-PE in a dose-dependent manner with estimated EC_{50} values at 8.54 µM, 3.45 µM, and
250 5.12 µM for HabiOR3, ItypOR6, and DponOR8^{HsCO}, respectively (Fig. 3B, D, F).
251

252 # Discussion

253 To allow for functional characterization of *H. abietis* ORs, antennal transcriptomes were
254 sequenced and the ORs annotated, suggesting a similarly sized OR repertoire (79 ORs) as in *I.*
255 *typographus* (73 ORs) and *D. ponderosae* (86 ORs) (Andersson, et al. 2019; Yuvaraj, et al.
256 2021). The largest number of HabiORs was found in OR Group 7, and *H. abietis* stands out
257 by its large OR-radiation within this group. This differs from both the bark beetles and the red
258 palm weevil *R. ferrugineus,* but displays similarity with the large radiation of Group 7 ORs in

259 the sweetpotato weevil *Cylas formicarius* (Antony, et al. 2016; Bin, et al. 2017). Our previous
260 study indicated that the two scolytine bark beetles *I. typographus* and *D. ponderosae* share 17
261 highly-supported simple OR orthologues (Yuvaraj, et al. 2021). Here, we included also the
262 pine weevil from the Molytinae subfamily in the analysis, and found that 12 simple
263 orthologues are conserved across these three species. The observation of fewer orthologues in
264 this broader analysis is consistent with the general positive correlation between species
265 relatedness and occurrence of OR orthology (Mitchell, et al. 2020). Our OR phylogeny also
266 support the notion that OR orthology is rare across beetle superfamilies (Mitchell and
267 Andersson 2020; Mitchell, et al. 2020).
268
269 To investigate whether OR orthologues are functionally conserved in the three curculionids,
270 and whether evolution of OR functionality may be traced beyond the beetle superfamily level,
271 we characterized two curculionid OR clades within beetle OR subfamily 2B, both of which
272 are evolutionarily related to the cerambycid 2-PE receptor McarOR5 (Mitchell, et al. 2012).
273 Our results show conserved functions across the tested OR orthologues, with one group
274 (HabiOR3/DponOR8/ItypOR6) responding exclusively to 2-PE, and the other group
275 (HabiOR4/DponOR9/ItypOR5) responding to several six-carbon GLV alcohols. Our results
276 further show that the 2-PE receptors in the curculionids share a common ancestor with
277 McarOR5, which is also the case for their GLV-responding ORs. Interestingly, the GLV
278 receptors in the curculionids are the most closely related to McarOR5, while their 2-PE
279 receptors are part of a sister clade. This suggests that the response to 2-PE may be ancestral
280 and that new functions such as GLV-responsiveness have subsequently evolved
281 (neofunctionalization) in the more recent OR lineages of the curculionids. Another possibility
282 would be that the ancestral receptor was broadly tuned to both 2-PE and GLVs and that the
283 more recent OR lineages, derived from gene duplication, may have evolved higher specificity
284 for either GLVs or 2-PE in the process of subfunctionalization (Andersson, et al. 2015). In
285 fact, this scenario may be supported by recent data from single-sensillum recordings (SSR)
286 from *I. typographus* showing secondary responses to 1-hexanol in the '2-PE' OSN class and
287 secondary responses to 2-PE in the 'GLV-OH' OSN class (Kandasamy, et al. 2019).
288 Revealing the responses of the remaining six related McarORs (McarORs 8, 10, 13, 22, 39,
289 and 56; see Figure 1) is needed to conclusively inform the evolutionary history of these OR
290 functions; in particular in this context, it could be enlightening to search for GLV-responding
291 ORs among the orphan McarORs. The clade containing the curculionid 2-PE receptors is also
292 intriguing due to the presence of orthologues in numerous additional species from several

293 beetle families, including *Anoplophora glabripennis* (Cerambycidae), *R. ferrugineus*
294 (Curculionidae), *Leptinotarsa decemlineata* (Chrysomelidae), *Tribolium castaneum*
295 (Tenebrionidae), *Nicrophorus vespilloides* (Silphidae), and *Onthophagus taurus*
296 (Scarabaeidae) (Mitchell, et al. 2020; Antony, et al. 2021). Unraveling the functions of the
297 orthologues in these species should inform how widely conserved the ORs for 2-PE are across
298 the Coleoptera. In moths, it was shown that OR orthologs detecting the flower compound
299 phenylacetaldehyde were functionally conserved across eleven species from several families
300 of the Glossata suborder although the majority of the other investigated orthologues were
301 functionally divergent, even among related species (Guo, Du, et al. 2021).
302
303 The strong functional conservation among the examined OR orthologues suggests that 2-PE
304 and GLV alcohols convey important fitness-related information to the three curculionids.
305 Indeed, GLVs are abundant in the leaves of angiosperms and less so in conifers, and are
306 regarded as non-host cues that typically inhibit the attraction of conifer-feeding bark beetles
307 to their aggregation pheromones (reviewed in Zhang and Schlyter 2004). Hence, GLVs are
308 likely used by the beetles to avoid colonizing angiosperm trees in which they cannot
309 reproduce (Dickens, et al. 1992; Schiebe, et al. 2011). A role of GLVs in host choice has also
310 been proposed for *H. abietis* (Pettersson, et al. 2008; Kännaste, et al. 2013). Extensive SSRs
311 from the OSNs of *I. typographus* have identified a single OSN class responding with similar
312 sensitivity to several GLV alcohols (*E*2-hexenol, *Z*3-hexenol, and 1-hexanol) (Andersson, et
313 al. 2009; Kandasamy, et al. 2019), which is in accordance with the data from the GLV-
314 responsive ORs characterized here. In *I. typographus*, the three GLVs have similar inhibitory
315 effects on pheromone attraction and the use of a single compound (e.g., 1-hexanol) can
316 replace a three-component GLV mixture at an equivalent release rate without compromising
317 the inhibitory effect (Zhang and Schlyter 2003; Unelius, et al. 2014). These findings support
318 the idea that this conifer specialist employs a single neuronal channel, hence likely a single
319 OR (ItypOR5), for the detection of several, structurally similar compounds that all convey the
320 message of a non-host plant that should be avoided (Andersson, et al. 2009; Raffa, et al.
321 2016). In *D. ponderosae*, coupled gas chromatographic-electroantennographic detection (GC-
322 EAD) demonstrated antennal detection of the GLV alcohols that activate DponOR9 (Wilson,
323 et al. 1996; Huber, et al. 2000). The strongest inhibitory effect on pheromone attraction was
324 observed for *Z*3-hexenol and *E*2-hexenol (Wilson, et al. 1996), that is, the two compounds
325 that elicited the strongest responses in DponOR9. However, since (to our knowledge) no
326 SSRs have been performed, it remains unknown whether *D. ponderosae* also has only a single

327 OSN class responding to six-carbon GLV compounds. Likewise, SSR studies testing GLV
328 compounds in *H. abietis* appear to be missing in the published literature (Wibe, et al. 1997).
329 In contrast to *I. typographus*, beetles feeding on angiosperms typically possess several OSN
330 classes detecting GLVs, each with their unique response specificity (Hansson, et al. 1999;
331 Larsson, et al. 2001; Andersson, et al. 2012; Carrasco, et al. 2019).
332
333 Also 2-PE is tightly connected to the chemical ecologies - and potentially reproductive fitness
334 - of the three investigated species. In *H. abietis* it is a potent anti-feedant, present in the gut of
335 the beetle and in non-host plants (Eriksson, et al. 2008; Axelsson, et al. 2017). Through
336 deposition of feces containing 2-PE over the laid eggs, the compound may contribute to
337 reducing egg predation by conspecifics (Borg-Karlson, et al. 2006; Axelsson, et al. 2017). It is
338 also present in the guts of both *D. ponderosae* and *I. typographus*. 2-PE inhibits attraction to
339 the aggregation pheromone in the former species, suggesting it may contribute to termination
340 of aggregation and induction of dispersal (Pureswaran, et al. 2000). In contrast, 2-PE appears
341 to have no effect on pheromone attraction in *I. typographus* (Schlyter, et al. 1987); however,
342 it is part of the odor blends released by several species of ophiostomatoid symbiotic fungi,
343 which are attractive to beetles in laboratory bioassays (Kandasamy, et al. 2019). These fungi,
344 inoculated by beetles inside their galleries under the tree bark, are likely to benefit beetles by
345 providing nutrients and through metabolism of the tree's chemical defenses (Kandasamy, et
346 al. 2019; Kandasamy, et al. 2021). *I. typographus* has an OSN class that primarily responds to
347 2-PE and secondarily to phenethyl acetate, 3-methyl-1-butanol and a few more compounds
348 (including 1-hexanol) with weaker activity (Kandasamy, et al. 2019). These secondary
349 responses were not evident in any of the three 2-PE receptors (HabiOR3, DponOR8, and
350 ItypOR6) characterized in the present study. Higher response specificities in ORs when tested
351 in HEK293 cells as compared to those seen in putatively corresponding OSN classes have
352 been observed also previously, such as for ItypOR46 and ItypOR49, responding to the beetle-
353 produced compounds ipsenol and ipsdienol, respectively (Yuvaraj, et al. 2021). Similarly,
354 several of the weakly active secondary compounds for the GLV-responsive OSN class in *I.*
355 *typographus*, including hexanal, *E*2-hexenal, 1-octen-3-ol, and 2-PE failed to activate
356 ItypOR5 (as well as DponOR9 and HabiOR4) (Andersson, et al. 2009; Kandasamy, et al.
357 2019). The reasons for this discrepancy remain unknown but could potentially be due to lower
358 sensitivity of the HEK cell assay as compared to SSR or a consequence of the "unnatural"
359 cellular environment in HEK cells, which may affect protein folding and hence access of
360 ligands to their binding sites (see also Hou, et al. 2020; Yuvaraj, et al. 2022).

361

362 In conclusion, we report the functional characterization of six ORs from three species of the
363 Curculionidae family, including the first characterized ORs from the devastating forest pests
364 *H. abietis* and *D. ponderosae.* We reveal highly conserved responses to ecologically relevant
365 odors within the two groups of assayed OR orthologues, suggesting that the detection of 2-PE
366 and GLVs is important for the fitness of conifer-feeding curculionids. The characterized ORs
367 were shown to be evolutionarily related with the 2-PE receptor in *M. caryae*, sharing a
368 common ancestral OR protein. Our findings demonstrating conserved responses among beetle
369 ORs from two taxonomic superfamilies provide new insight into the functional evolution of
370 the OR family in this large insect order.
371

372 Materials and Methods

373 ***Sequencing, assembly, annotation, and analyses of the* Hylobius abietis *antennal***
374 ***transcriptome***

375 Wild beetles were collected by hand at Balungstrand's sawmill in Enviken, close to Falun in
376 mid-Sweden, and kindly provided by Prof. Göran Nordlander (Swedish University of
377 Agricultural Sciences, Uppsala, Sweden). The antennae from 20 males and 20 females were
378 excised and collected separately in tubes kept on dry ice and then stored at −80 °C. The
379 antennae were homogenized using Tissue-tearor model 98370-365 (Bartlesville, OK, USA),
380 and total RNA was isolated using the RNeasy Minikit (Qiagen, Hilden, Germany).
381 Extractions yielded 4.8 µg and 3.1 µg of high-quality total RNA from male and female
382 antennal samples, respectively. These RNA samples were used for both transcriptome
383 sequencing and molecular cloning.
384

385 The RNA samples were DNase-treated and then underwent poly-A enrichment and library
386 construction using a TruSeq v2 Library Preparation Kit (Illumina, San Diego, CA, USA),
387 followed by 150 bp paired-end sequencing on an Illumina HiSeq 3000 platform at the Max
388 Planck-Genome center (Cologne, Germany). The sequencing produced 36,455,021 and
389 35,770,733 paired-end reads from the male and female samples, respectively. Adaptor
390 sequences and low-quality reads were removed using Trimmomatic (v 0.36) (Bolger, et al.
391 2014) with a custom screening database, before performing *de novo* assemblies with Trinity
392 version 2.4.0 (Grabherr, et al. 2011). Reads from males and females were assembled
393 separately, and also combined. Contigs from the Trinity output were clustered to reduce the

394 number of redundant transcripts using CD-HIT-EST (v 4.6.8) (Li and Godzik 2006) with a
395 sequence identity threshold of 0.98. Primarily, the sex-combined non-redundant assembly was
396 used for downstream annotation of OR-encoding transcripts, and was comprised of 46,669
397 predicted protein-coding 'genes' with their respective isoforms and together with other non-
398 coding genes totaled 199,035 transcripts. The average transcript length was 824 bp with an
399 N50 of 1,570 bp. The completeness of the sex-combined assembly was firstly assessed using
400 the Benchmarking Universal Single-Copy Orthologs (BUSCO v5.2.2;
401 https://busco.ezlab.org/) tool performed against the Insecta odb10 dataset, including 1,367
402 reference genes (Manni, et al. 2021). This analysis revealed 96.6% complete (C) BUSCOs, of
403 which 59.8% were present as single copy genes (S) and 40.2% as duplicated genes (D). Only
404 30 (2.3%) BUSCOs were missing (M) from the assembly and 17 (1.3%) BUSCOs were
405 fragmented (F), indicating the majority of transcripts were represented and were full length.
406 Mapping of the clean reads to the non-redundant assembly resulted in an overall alignment
407 rate of 94.06%, further demonstrating a high level of completeness for this assembly. The
408 RNAseq reads have been deposited in the SRA database at NCBI under the BioProject
409 accession number PRJNA783427.
410
411 *H. abietis* OR genes were annotated through exhaustive tBLASTn searches against the
412 assemblies at an *e*-value cut-off at 1.0. The OR query sequences were obtained from *I.*
413 *typographus* (Andersson, et al. 2013; Yuvaraj, et al. 2021), *D. ponderosae* (Andersson, et al.
414 2013; Andersson, et al. 2019), *Anoplophora glabripennis* (McKenna, et al. 2016), *M. caryae*
415 (Mitchell, et al. 2012), and *Leptinotarsa decemlineata* (Schoville, et al. 2018). All annotated
416 HabiOR sequences were included in additional tBLASTn searches against the *H. abietis*
417 assemblies until all novel OR hits were exhausted. Except for the HabiOrco gene which was
418 only assembled to full length in the male-specific assembly, all OR genes were annotated
419 from the sex-combined assembly, and no OR genes were uniquely found or assembled to
420 higher completeness in the two sex-specific assemblies. A few partial OR genes could be
421 extended by joining overlapping transcripts with identical sequences. The names of these
422 genes were given a 'JOI' suffix according to established nomenclature (Andersson, et al.
423 2019, and references therein). Likewise, OR genes missing the N-terminus or C-terminus
424 were given the suffixes 'NTE' and 'CTE', respectively, to their names. Single letter
425 abbreviations were used in combinations (i.e., J, N, C) for genes with multiple suffixes.
426 Transcripts encoding partial OR sequences below 170 amino acids and those that that did not
427 overlap with other OR sequences in multiple sequence alignments were discarded as they may

428 not represent unique genes. Likewise, for ORs sharing >96% amino acid identity, only one
429 transcript was kept in the dataset to exclude potential assembly isoforms or allelic variants.
430 The identified HabiOR genes were given names from HabiOR1 to HabiOR78 following their
431 groupings in the OR phylogeny (Fig. 1), with consecutive numbering within the major
432 coleopteran OR clades (Mitchell, et al. 2020).
433
434 To analyze the expression levels of OR genes in male and female antennae, clean reads were
435 mapped to the ORFs of annotated HabiOR genes using the align_and_estimate_abundance.pl
436 script from the Trinity v2.4.0 software package (Haas, et al. 2013) with default parameters
437 except for --est_method RSEM--aln_method bowtie2 --trinity_mode. The rationale for
438 mapping to the ORFs of OR genes, and not to all transcripts in the assembly, was because
439 some OR transcripts contained misassembled fragments in non-coding regions, which could
440 bias the estimated expression level of the OR gene.
441
442 The HabiOR amino acid sequences were aligned with the OR sequences from *D. ponderosae*
443 (Andersson, et al. 2019), *I. typographus* (Yuvaraj, et al. 2021), and *M. caryae* (Mitchell, et al.
444 2012) using MAFFT v7.450 (Katoh, et al. 2002; Katoh and Standley 2013), implemented in
445 Geneious Prime v.2020.0.5 (Biomatters Ltd. Auckland, New Zealand). The alignment of a
446 few partial OR sequences were corrected manually. Three miss-aligned partial McarOR
447 sequences (McarORs 41PAR, 50PAR, and 53PAR) were excluded from analysis since their
448 alignments could not be corrected with confidence. Uninformative regions were excised using
449 trimAl v.1.2 (Capella-Gutiérrez, et al. 2009) with the following settings: similarity threshold
450 0, gap threshold 0.7, and minimum 25% conserved positions. The trimmed alignment was
451 used to construct a phylogenetic tree of ORs using FastTree v.2.1.11 at default settings (Price,
452 et al. 2010). Local node support values were calculated using the Shimodaira-Hasegawa (SH)
453 test implemented within FastTree. The tree was rooted with the Orco lineage, and color coded
454 in FigTree v.1.4.3 (Rambaut 2014). Final graphical editing was performed using Adobe
455 Illustrator.
456
457 ***Molecular cloning and generation of HEK293 cell lines***
458 The protocols for cloning, cell line generation, and culturing have been previously described
459 (Corcoran, et al. 2014; Andersson, et al. 2016; Yuvaraj, et al. 2021). Briefly, OR (and Orco)
460 genes with added 5' Apa1 and 3' Not1 restriction sites, *cacc* Kozak sequence, and N-terminal
461 epitope tags (Myc for Orco, V5 for ORs) were ligated into the pcDNATM4/TO (Orco) or

462 pcDNATM5/TO (ORs) mammalian expression vectors (Thermo Fisher Scientific). For OR
463 genes that required codon optimization for functional expression in HEK293 cells (Roberts, et
464 al. 2021), the nucleotide sequences were submitted to the Thermo Fisher Scientific GeneArt
465 Portal and codon optimized for *Homo sapiens*, excluding the start methionine and the epitope
466 tag, then synthesized and ligated into the pcDNATM5/TO expression vector. Because we had
467 no access to biological material from *D. ponderosae*, the two functionally assayed DponOR
468 genes were synthesized as codon optimized versions directly, and also because several
469 wildtype beetle OR genes are not functionally expressed in HEK cells (Roberts, et al. 2021).
470 A codon optimized gene of HabiOR4 was also tested since Western blots (below) failed to
471 detect this protein from cells transfected with the wildtype gene. Sequences of codon
472 optimized genes from the two species are provided in Supplementary Table 2. Sequences of
473 OR genes cloned from antennal cDNA (ItypOR5, ItypOR6, HabiOR3, and HabiOR4) have
474 been deposited in GenBank under the accession numbers OL865310-OL865313.
475
476 OR genes in expression vectors were transformed into HB101 ampicillin-resistant competent
477 cells (Promega), plated on ampicillin-containing agar, and incubated overnight at 37 °C.
478 Resulting colonies were PCR-screened with vector-specific primers, spread onto a new plate,
479 and incubated at 37 °C for 4-6 hours. Positive colonies were sub-cultured overnight at 37°C in
480 LB broth containing ampicillin. Plasmid DNA from the overnight cultures was harvested via
481 extraction with the PureLinkTM HiPure Plasmid Filter Midiprep kit (Thermo Fisher
482 Scientific), and insert sequence was confirmed by Sanger sequencing at the on-site DNA
483 Sequencing Facility (Dept. Biology, Lund University) using the BigDye® Terminator v1.1
484 Cycle Sequencing Kit (Thermo Fisher Scientific). Positive plasmids were linearized with
485 FspI, PciI, or BstZ17I (New England Biolabs, Ipswich, MA, United States) restriction
486 enzymes and incubated overnight at 37 °C.
487
488 Linearized plasmids containing the ItypOrco gene were transfected into HEK293 cells
489 containing a tetracycline-inducible repressor (TREx) using Lipofectamine 2000 (Thermo
490 Fisher Scientific) (Corcoran, et al. 2014). Twenty-four hours post-transfection, antibiotics
491 (blasticidin for TREx, zeocin for Orco; both NEB) were added to select successfully
492 transfected cells. Once a stable cell line was generated, protein expression of the ItypOrco
493 gene was confirmed via Western blot analysis and functionality of Orco was confirmed using
494 the Orco agonist VUAA1 (described below) (Jones, et al. 2011). We recently found that the
495 DponOrco gene is not functionally expressed in HEK cells (Roberts, et al. 2021); we

496 therefore co-expressed the DponOR genes with the ItypOrco gene to allow functional
497 characterization of these ORs. For consistency, the HabiOR genes were also tested together
498 with the ItypOrco. Due to the conserved function of Orco and the relatedness among the three
499 beetle species, we assumed that this strategy would not affect the OR response specificities.
500 This assumption is supported by previous studies showing that combinations of OR and Orco
501 proteins from different taxa assemble into functional receptor complexes responding properly
502 to known ligands (Corcoran, et al. 2018). The linearized OR gene-containing plasmids were
503 transfected into the stably expressing TREx/ItypOrco cell line as described above, and
504 cultured with the antibiotic hygromycin (Gold BioTech) to select successfully transfected
505 cells. Resulting cell lines were frozen at –80 °C before functional assays.
506
507 ***Protein extraction and Western blot analysis***
508 Cells were cultured without antibiotics for 24 hours before the expression of Orco and OR
509 genes was induced with doxycycline (Sigma). At 16 hours post-induction, cells were pelleted
510 via centrifugation and total protein extraction was performed as described by Corcoran et al.
511 (2014). Protein extractions from non-induced cells served as negative controls. Western blot
512 was performed using 25 µg of total protein from each sample and standard protocols for
513 mixed molecular weight proteins. Primary antibodies (rabbit anti-Myc for Orco, rabbit anti-
514 V5 for ORs) were added at a ratio of 1:2000, and the secondary antibody (anti-rabbit +IgG,
515 HRP-linked for both Orco and ORs) was added at a ratio of 1:5000 (all antibodies from Cell
516 Signaling Technology), as described by Andersson et al. (2016).
517
518 ***Functional characterization of odorant receptors***
519 Ligand-binding activity of cell lines co-expressing Orco and ORs was tested via a calcium
520 fluorescence assay using a CLARIOstar Omega plate reader (BMG Labtech, Ortenberg,
521 Germany) according to previously described protocols (Corcoran, et al. 2014; Andersson, et
522 al. 2016; Yuvaraj, et al. 2021). Briefly, cells were plated in black-walled poly-D-lysine coated
523 96-well plates (Corning Costar) and incubated overnight. Cells in half the wells were treated
524 with doxycycline to induce expression of exogenous Orco and OR genes 16 hours prior to
525 testing, leaving the non-induced cells as negative controls. The calcium-sensitive fluorophore
526 Fluo-4AM (Life Technologies) was loaded into all wells, and plates were incubated in the
527 dark at room temperature for 30 min before being washed with assay buffer, then incubated
528 for another 30 min in the dark at room temperature prior to the assay.
529

530 The test odor panel included 62 compounds (Supplementary Table 3) that are ecologically
531 relevant for conifer-feeding curculionids, including pheromone compounds, volatiles from
532 conifers and angiosperms as well as odorants produced by bark beetle fungal symbionts
533 (Kandasamy, et al. 2019; Kandasamy, et al. 2021; Yuvaraj, et al. 2021). The Orco agonist
534 VUAA1 was tested (at 50 μM) on each cell line as a positive control for functional Orco
535 expression. Test odors were diluted in DMSO and assay buffer with a final concentration of
536 30 μM in the plate wells for screening experiments. Compounds were tested over a minimum
537 of three biological replicates (plates), and were pipetted into three induced and three non-
538 induced wells per plate, creating three technical replicates per plate. A negative control of
539 0.5% DMSO in assay buffer (vehicle) was tested on each cell line. Background fluorescence
540 was measured for both induced and non-induced cells immediately before compounds were
541 added to the wells, with ligand-binding response of cells measured as the percentage increase
542 in fluorescence from background readings 10 s post stimulation. Mean responses of cells to
543 the added ligands were calculated using GraphPad Prism 6 (GraphPad Software Inc., La Jolla,
544 CA, United States).
545
546 A response of ≥1% increase in fluorescence in induced cells was required for a compound to
547 be considered active, provided a significantly higher response in induced compared to non-
548 induced cells. Hence, a general linear model (GLM) with "induction" as a fixed factor and
549 "plate" as a random factor (to account for inter-plate variation) was performed using IBM
550 SPSS statistics v.25. Bonferroni correction to maintain the α-level at 0.05 (for up to 12
551 multiple comparisons within a cell line) was undertaken to avoid reporting false positives
552 (Type I statistical error). Compounds eliciting an increase in fluorescence of 3% or more at
553 the 30 μM screening concentration were tested in subsequent dose-response experiments.
554 Half-maximal effective concentrations (EC_{50}) were calculated using the non-linear curve fit
555 regression function in GraphPad Prism (version 6). Calculations of EC_{50} values were only
556 performed for compounds with (reasonably) sigmoid dose-response curves.
557

558 # Acknowledgements

559 We thank Göran Nordlander for providing pine weevils for RNA extractions. We thank
560 Rikard Unelius, Suresh Ganji, Erika Wallin, Blanka Kalinová, Fredrik Schlyter, Anna
561 Jirošová, and Wittko Francke for providing compounds. Caroline Isaksson is acknowledged
562 for hosting of DP. The study was funded by grants from the Swedish Research Councils

FORMAS (grant numbers 217-2014-689 and 2018-01444 to MNA; grant number 2018-01630 to JKY) and VR (grant number 2017-03804 to CL), the Crafoord Foundation (to MNA), the Carl Trygger Foundation (grant number CTS 17:25 to MNA), the Royal Physiographic Society in Lund (to RER, TB, and MNA), the Foundation in Memory of Oscar and Lili Lamm (to MNA), and the Max Planck Society (to EG-W and BSH).

Author contributions

MNA conceived the project. RER and MNA conceptualized and designed the study. RER, TB, JKY, and MNA performed molecular work. RER, TB, and JKY performed cell culturing and experimental assays. EG-W, BSH, and MNA coordinated the sequencing of *H. abietis*. EG-W and DP performed transcriptome assemblies, with DP assessing OR gene expression and completeness of final assemblies. MNA annotated the HabiORs, constructed the OR phylogeny, and performed statistical analysis of the HEK cell data. MNA, JKY, and CL contributed to project supervision. MNA and RER drafted the manuscript. All authors contributed to the final version of the manuscript, and have read and approved it for submission.

Data availability

The *H. abietis* RNAseq reads have been deposited in the SRA database at NCBI under the BioProject accession number PRJNA783427. Sequences of cloned OR genes ItypOR5, ItypOR6, HabiOR3, and HabiOR4 have been deposited in GenBank under the accession numbers OL865310-OL865313. Raw data from all HEK cell assays are reported in the supplementary materials of this article.

References

Andersson MN, Corcoran JA, Zhang D-D, Hillbur Y, Newcomb RD, Löfstedt C. 2016. A sex pheromone receptor in the Hessian fly *Mayetiola destructor* (Diptera, Cecidomyiidae). *Front Cell Neurosci.* 10:212.

Andersson MN, Grosse-Wilde E, Keeling CI, Bengtsson JM, Yuen MM, Li M, Hillbur Y, Bohlmann J, Hansson BS, Schlyter F. 2013. Antennal transcriptome analysis of the chemosensory gene families in the tree killing bark beetles, *Ips typographus* and *Dendroctonus ponderosae* (Coleoptera: Curculionidae: Scolytinae). *BMC Genomics.* 14:198.

596 Andersson MN, Keeling CI, Mitchell RF. 2019. Genomic content of chemosensory genes
597 correlates with host range in wood-boring beetles (*Dendroctonus ponderosae*, *Agrilus*
598 *planipennis*, and *Anoplophora glabripennis*). *BMC Genomics.* 20:690.
599 Andersson MN, Larsson MC, Schlyter F. 2009. Specificity and redundancy in the olfactory
600 system of the bark beetle *Ips typographus*: Single-cell responses to ecologically relevant
601 odors. *J Insect Physiol.* 55:556-567.
602 Andersson MN, Larsson MC, Svensson GP, Birgersson G, Rundlöf M, Lundin O, Lankinen
603 Å, Anderbrant O. 2012. Characterization of olfactory sensory neurons in the white
604 clover seed weevil, *Apion fulvipes* (Coleoptera: Apionidae). *J Insect Physiol.* 58:1325-
605 1333.
606 Andersson MN, Löfstedt C, Newcomb RD. 2015. Insect olfaction and the evolution of
607 receptor tuning. *Front Ecol Evol.* 3:53.
608 Antony B, Johny J, Montagné N, Jacquin-Joly E, Capoduro R, Cali K, Persaud K, Al-Saleh
609 MA, Pain A. 2021. Pheromone receptor of the globally invasive quarantine pest of the
610 palm tree, the red palm weevil (*Rhynchophorus ferrugineus*). *Mol Ecol.* 30:2025-2039.
611 Antony B, Soffan A, Jakše J, Abdelazim MM, Aldosari SA, Aldawood AS, Pain A. 2016.
612 Identification of the genes involved in odorant reception and detection in the palm
613 weevil *Rhynchophorus ferrugineus*, an important quarantine pest, by antennal
614 transcriptome analysis. *BMC Genomics.* 17:69.
615 Axelsson K, Konstanzer V, Rajarao GK, Terenius O, Seriot L, Nordenhem H, Nordlander G,
616 Borg-Karlson A-K. 2017. Antifeedants produced by bacteria associated with the gut of
617 the pine weevil *Hylobius abietis*. *Microb Ecol.* 74:177-184.
618 Benton R. 2015. Multigene family evolution: perspectives from insect chemoreceptors.
619 *Trends Ecol Evol.* 30:590-600.
620 Bin S-Y, Qu M-Q, Pu X-H, Wu Z-Z, Lin J-T. 2017. Antennal transcriptome and expression
621 analyses of olfactory genes in the sweetpotato weevil *Cylas formicarius*. *Sci Rep.*
622 7:11073.
623 Birgersson G, Schlyter F, Löfqvist J, Bergström G. 1984. Quantitative variation of pheromone
624 components in the spruce bark beetle *Ips typographus* from different attack phases. *J*
625 *Chem Ecol.* 10:1029-1055.
626 Bolger AM, Lohse M, Usadel B. 2014. Trimmomatic: a flexible trimmer for Illumina
627 sequence data. *Bioinformatics.* 30:2114-2120.

628 Borg-Karlson A-K, Nordlander G, Mudalige A, Nordenhem H, Unelius CR. 2006.
629 Antifeedants in the feces of the pine weevil *Hylobius abietis*: identification and
630 biological activity. *J Chem Ecol.* 32:943-957.
631 Brand P, Ramírez SR. 2017. The evolutionary dynamics of the odorant receptor gene family
632 in corbiculate bees. *Genome Biol Evol.* 9:2023-2036.
633 Brand P, Robertson HM, Lin W, Pothula R, Klingeman WE, Jurat-Fuentes JL, Johnson BR.
634 2018. The origin of the odorant receptor gene family in insects. *eLife.* 7:e38340.
635 Butterwick JA, del Mármol J, Kim KH, Kahlson MA, Rogow JA, Walz T, Ruta V. 2018.
636 Cryo-EM structure of the insect olfactory receptor Orco. *Nature.* 560:447-452.
637 Capella-Gutiérrez S, Silla-Martínez JM, Gabaldón T. 2009. trimAl: a tool for automated
638 alignment trimming in large-scale phylogenetic analyses. *Bioinformatics.* 25:1972-
639 1973.
640 Carrasco D, Nyabuga FN, Anderbrant O, Svensson GP, Birgersson G, Lankinen Å, Larsson
641 MC, Andersson MN. 2019. Characterization of olfactory sensory neurons in the red
642 clover seed weevil, *Protapion trifolii* (Coleoptera: Brentidae) and comparison to the
643 closely related species *P. fulvipes*. *J Insect Physiol.* 119:103948.
644 Clyne PJ, Warr CG, Freeman MR, Lessing D, Kim J, Carlson JR. 1999. A novel family of
645 divergent seven-transmembrane proteins: candidate odorant receptors in *Drosophila*.
646 *Neuron.* 22:327-338.
647 Corcoran JA, Jordan MD, Carraher C, Newcomb RD. 2014. A novel method to study insect
648 olfactory receptor function using HEK293 cells. *Insect Biochem Mol Biol.* 54:22-32.
649 Corcoran JA, Sonntag Y, Andersson MN, Johanson U, Löfstedt C. 2018. Endogenous
650 insensitivity to the Orco agonist VUAA1 reveals novel olfactory receptor complex
651 properties in the specialist fly *Mayetiola destructor*. *Sci Rep.* 8:3489.
652 Dahanukar A, Hallem EA, Carlson JR. 2005. Insect chemoreception. *Curr Opin Neurobiol.*
653 15:423-430.
654 Dekel A, Pitts RJ, Yakir E, Bohbot JD. 2016. Evolutionarily conserved odorant receptor
655 function questions ecological context of octenol role in mosquitoes. *Sci Rep.* 6:37330.
656 Dickens JC, Billings RF, Payne TL. 1992. Green leaf volatiles interrupt aggregation
657 pheromone response in bark beetles infesting southern pines. *Experientia.* 48:523-524.
658 Eriksson C, Månsson PE, Sjödin K, Schlyter F. 2008. Antifeedants and feeding stimulants in
659 bark extracts of ten woody non-host species of the pine weevil, *Hylobius abietis*. *J*
660 *Chem Ecol.* 34:1290-1297.

661 Gonzalez F, Bengtsson JM, Walker WB, Sousa MF, Cattaneo AM, Montagné N, de Fouchier
662 A, Anfora G, Jacquin-Joly E, Witzgall P. 2015. A conserved odorant receptor detects
663 the same 1-indanone analogs in a tortricid and a noctuid moth. *Front Ecol Evol.* 3:131.
664 Grabherr MG, Haas BJ, Yassour M, Levin JZ, Thompson DA, Amit I, Adiconis X, Fan L,
665 Raychowdhury R, Zeng Q. 2011. Full-length transcriptome assembly from RNA-Seq
666 data without a reference genome. *Nat Biotechnol.* 29:644.
667 Guo H, Huang L-Q, Gong X-L, Wang C-Z. 2021. Comparison of functions of pheromone
668 receptor repertoires in *Helicoverpa armigera* and *Helicoverpa assulta* using a
669 Drosophila expression system. *Insect Biochem Mol Biol.* 141:103702.
670 Guo M, Du L, Chen Q, Feng Y, Zhang J, Zhang X, Tian K, Cao S, Huang T, Jacquin-Joly E,
671 et al. 2021. Odorant receptors for detecting flowering plant cues are functionally
672 conserved across moths and butterflies. *Mol Biol Evol.* 38:1413–1427.
673 Haas BJ, Papanicolaou A, Yassour M, Grabherr M, Blood PD, Bowden J, Couger MB, Eccles
674 D, Li B, Lieber M, et al. 2013. *De novo* transcript sequence reconstruction from RNA-
675 seq using the Trinity platform for reference generation and analysis. *Nat Protoc.*
676 8:1494-1512.
677 Hansson BS, Larsson MC, Leal WS. 1999. Green leaf volatile-detecting olfactory receptor
678 neurones display very high sensitivity and specificity in a scarab beetle. *Physiol*
679 *Entomol.* 24:121-126.
680 Hansson BS, Stensmyr MC. 2011. Evolution of insect olfaction. *Neuron.* 72:698-711.
681 Hou X, Zhang D-D, Yuvaraj JK, Corcoran JA, Andersson MN, Löfstedt C. 2020. Functional
682 characterization of odorant receptors from the moth *Eriocrania semipurpurella*: a
683 comparison of results in the *Xenopus* oocyte and HEK cell systems. *Insect Biochem Mol*
684 *Biol.* 117:103289.
685 Hou X-Q, Yuvaraj JK, Roberts RE, Zhang D-D, Unelius CR, Löfstedt C, Andersson MN.
686 2021. Functional evolution of a bark beetle odorant receptor clade detecting
687 monoterpenoids of different ecological origins. *Mol Biol Evol.* 38:4934-4947.
688 Huber DPW, Gries R, Borden JH, Pierce Jr HD. 2000. A survey of antennal responses by five
689 species of coniferophagous bark beetles (Coleoptera: Scolytidae) to bark volatiles of six
690 species of angiosperm trees. *Chemoecology.* 10:103-113.
691 Ji T, Xu Z, Jia Q, Wang G, Hou Y. 2021. Non-palm plant volatile α-pinene is detected by
692 antenna-biased expressed odorant receptor 6 in the *Rhynchophorus ferrugineus*
693 (Olivier)(Coleoptera: Curculionidae). *Front Physiol.*1187.

694 Jones PL, Pask GM, Rinker DC, Zwiebel LJ. 2011. Functional agonism of insect odorant
695 receptor ion channels. *Proc Natl Acad Sci USA.* 108:8821-8825.
696 Kandasamy D, Gershenzon J, Andersson MN, Hammerbacher A. 2019. Volatile organic
697 compounds influence the interaction of the Eurasian spruce bark beetle (*Ips*
698 *typographus*) with its fungal symbionts. *ISME J.* 13:1788–1800.
699 Kandasamy D, Zaman R, Nakamura Y, Zhao T, Hartmann H, Andersson MN, Hammerbacher
700 A, Gershenzon J. 2021. Bark beetles locate fungal symbionts by detecting volatile
701 fungal metabolites of host tree resin monoterpenes. *bioRxiv.*
702 https://doi.org/10.1101/2021.1107.1103.450988, last accessed 22 February 2022.
703 Katoh K, Misawa K, Kuma Ki, Miyata T. 2002. MAFFT: a novel method for rapid multiple
704 sequence alignment based on fast Fourier transform. *Nucleic Acids Res.* 30:3059-3066.
705 Katoh K, Standley DM. 2013. MAFFT multiple sequence alignment software version 7:
706 improvements in performance and usability. *Mol Biol Evol.* 30:772-780.
707 Kännaste A, Zhao T, Lindström A, Stattin E, Långström B, Borg-Karlson A-K. 2013. Odors
708 of Norway spruce (Picea abies L.) seedlings: differences due to age and chemotype.
709 *Trees.* 27:149-159.
710 Larsson MC, Domingos AI, Jones WD, Chiappe ME, Amrein H, Vosshall LB. 2004. Or83b
711 encodes a broadly expressed odorant receptor essential for *Drosophila* olfaction.
712 *Neuron.* 43:703-714.
713 Larsson MC, Leal WS, Hansson BS. 2001. Olfactory receptor neurons detecting plant odours
714 and male volatiles in *Anomala cuprea* beetles (Coleoptera: Scarabaeidae). *J Insect*
715 *Physiol.* 47:1065-1076.
716 Leufvén A, Bergström G, Falsen E. 1984. Interconversion of verbenols and verbenone by
717 identified yeasts isolated from the spruce bark beetle *Ips typographus*. *J Chem Ecol.*
718 10:1349-1361.
719 Li W, Godzik A. 2006. Cd-hit: a fast program for clustering and comparing large sets of
720 protein or nucleotide sequences. *Bioinformatics.* 22:1658-1659.
721 Manni M, Berkeley MR, Seppey M, Zdobnov EM. 2021. BUSCO: Assessing genomic data
722 quality and beyond. *Curr Protoc.* 1:e323.
723 McKenna DD, Scully ED, Pauchet Y, Hoover K, Kirsch R, Geib SM, Mitchell RF,
724 Waterhouse RM, Ahn S-J, Arsala D. 2016. Genome of the Asian longhorned beetle
725 (*Anoplophora glabripennis*), a globally significant invasive species, reveals key
726 functional and evolutionary innovations at the beetle–plant interface. *Genome Biol.*
727 17:227.

728 Mitchell RF, Andersson MN. 2020. Olfactory genomics of the Coleoptera. In: Blomquist GJ,
729 Vogt RG, editors. Insect Pheromone Biochemistry and Molecular Biology 2nd Edition.
730 Oxford: Academic Press. p. 547-590.
731 Mitchell RF, Hughes DT, Luetje CW, Millar JG, Soriano-Agatón F, Hanks LM, Robertson
732 HM. 2012. Sequencing and characterizing odorant receptors of the cerambycid beetle
733 *Megacyllene caryae*. *Insect Biochem Mol Biol.* 42:499-505.
734 Mitchell RF, Schneider TM, Schwartz AM, Andersson MN, McKenna DD. 2020. The
735 diversity and evolution of odorant receptors in beetles (Coleoptera). *Insect Mol Biol.*
736 29:77-91.
737 Nei M, Niimura Y, Nozawa M. 2008. The evolution of animal chemosensory receptor gene
738 repertoires: roles of chance and necessity. *Nat Rev Genet.* 9:951-963.
739 Pettersson M, Kännaste A, Lindström A, Hellqvist C, Stattin E, Långström B, Borg-Karlson
740 A-K. 2008. Mini-seedlings of *Picea abies* are less attacked by *Hylobius abietis* than
741 conventional ones: is plant chemistry the explanation? *Scand J For Res.* 23:299-306.
742 Price MN, Dehal PS, Arkin AP. 2010. FastTree 2–approximately maximum-likelihood trees
743 for large alignments. *PloS one.* 5:e9490.
744 Pureswaran DS, Gries R, Borden JH, Pierce Jr HD. 2000. Dynamics of pheromone production
745 and communication in the mountain pine beetle, *Dendroctonus ponderosae* Hopkins,
746 and the pine engraver, *Ips pini* (Say)(Coleoptera: Scolytidae). *Chemoecology.* 10:153-
747 168.
748 Raffa KF, Andersson MN, Schlyter F. 2016. Chapter one-Host selection by bark beetles:
749 Playing the odds in a high-stakes game. In: Tittiger C, Blomquist GJ, editors. Adv
750 Insect Physiol. Oxford: Academic press. Vol 50. p. 1-74.
751 Rambaut A. 2014. FigTree v1.4.0, a graphical viewer of phylogenetic trees.
752 http://tree.bio.ed.ac.uk/software/figtree/
753 Roberts RE, Yuvaraj JK, Andersson MN. 2021. Codon optimization of insect odorant
754 receptor genes may increase their stable expression for functional characterization in
755 HEK293 cells. *Front Cell Neurosci.* 15:744401.
756 Ruel DM, Yakir E, Bohbot JD. 2019. Supersensitive odorant receptor underscores pleiotropic
757 roles of indoles in mosquito ecology. *Front Cell Neurosci.* 12:533.
758 Sato K, Pellegrino M, Nakagawa T, Vosshall LB, Touhara K. 2008. Insect olfactory receptors
759 are heteromeric ligand-gated ion channels. *Nature.* 452:1002-1006.
760 Schiebe C, Blaženec M, Jakuš R, Unelius CR, Schlyter F. 2011. Semiochemical diversity
761 diverts bark beetle attacks from Norway spruce edges. *J Appl Entomol.* 135:726-737.

762 Schlyter F, Birgersson G, Byers JA, Löfqvist J, Bergström G. 1987. Field response of spruce
763 bark beetle, *Ips typographus*, to aggregation pheromone candidates. *J Chem Ecol.*
764 13:701-716.
765 Schoville SD, Chen YH, Andersson MN, Benoit JB, Bhandari A, Bowsher JH, Brevik K,
766 Cappelle K, Chen M-JM, Childers A, et al. 2018. A model species for agricultural pest
767 genomics: the genome of the Colorado potato beetle, *Leptinotarsa decemlineata*
768 (Coleoptera: Chrysomelidae). *Sci Rep.* 8:1931.
769 Shin S, Clarke DJ, Lemmon AR, Moriarty Lemmon E, Aitken AL, Haddad S, Farrell BD,
770 Marvaldi AE, Oberprieler RG, McKenna DD. 2018. Phylogenomic data yield new and
771 robust insights into the phylogeny and evolution of weevils. *Mol Biol Evol.* 35:823-836.
772 Stensmyr MC, Dweck HKM, Farhan A, Ibba I, Strutz A, Mukunda L, Linz J, Grabe V, Steck
773 K, Lavista-Llanos S, et al. 2012. A conserved dedicated olfactory circuit for detecting
774 harmful microbes in *Drosophila*. *Cell.* 151:1345-1357.
775 Sullivan BT. 2005. Electrophysiological and behavioral responses of *Dendroctonus frontalis*
776 (Coleoptera: Curculionidae) to volatiles isolated from conspecifics. *J Econ Entomol.*
777 98:2067-2078.
778 Unelius RC, Schiebe C, Bohman B, Andersson MN, Schlyter F. 2014. Non-host volatile
779 blend optimization for forest protection against the European spruce bark beetle, *Ips*
780 *typographus*. *PLoS ONE.* 9:e85381.
781 Vosshall L, Amrein H, Morozov P, Rzhetsky A, Axel R. 1999. A spatial map of olfactory
782 receptor expression in the *Drosophila* antenna. *Cell.* 96:725-736.
783 Wang X, Wang S, Yi J, Li Y, Liu J, Wang J, Xi J. 2020. Three host plant volatiles, hexanal,
784 lauric acid, and tetradecane, are detected by an antenna-biased expressed odorant
785 receptor 27 in the dark black chafer *Holotrichia parallela*. *J Agric Food Chem.*
786 68:7316-7323.
787 Wibe A, Borg-Karlson A-K, Norin T, Mustaparta H. 1997. Identification of plant volatiles
788 activating single receptor neurons in the pine weevil (*Hylobius abietis*). *J Comp Physiol*
789 *A.* 180:585-595.
790 Wicher D, Schäfer R, Bauernfeind R, Stensmyr MC, Heller R, Heinemann SH, Hansson BS.
791 2008. *Drosophila* odorant receptors are both ligand-gated and cyclic-nucleotide-
792 activated cation channels. *Nature.* 452:1007-1011.
793 Wilson IM, Borden JH, Gries R, Gries G. 1996. Green leaf volatiles as antiaggregants for the
794 mountain pine beetle, *Dendroctonus ponderosae* Hopkins (Coleoptera: Scolytidae). *J*
795 *Chem Ecol.* 22:1861-1875.

Xie J, Liu T, Yi C, Liu X, Tang H, Sun Y, Shi W, Khashaveh A, Zhang Y. 2022. Antenna-biased odorant receptor HvarOR25 in *Hippodamia variegata* tuned to allelochemicals from hosts and habitat involved in perceiving preys. *J Agric Food Chem.* 70:1090-1100.

Yuvaraj JK, Jordan MD, Zhang D-D, Andersson MN, Löfstedt C, Newcomb RD, Corcoran JA. 2022. Sex pheromone receptors of the light brown apple moth, *Epiphyas postvittana*, support a second major pheromone receptor clade within the Lepidoptera. *Insect Biochem Mol Biol.* 141:103708.

Yuvaraj JK, Roberts RE, Sonntag Y, Hou X, Grosse-Wilde E, Machara A, Zhang D-D, Hansson BS, Johanson U, Löfstedt C, et al. 2021. Putative ligand binding sites of two functionally characterized bark beetle odorant receptors. *BMC Biol.* 19:16.

Zhang Q-H, Schlyter F. 2004. Olfactory recognition and behavioural avoidance of angiosperm nonhost volatiles by conifer-inhabiting bark beetles. *Agric For Entomol.* 6:1-19.

Zhang Q-H, Schlyter F. 2003. Redundancy, synergism, and active inhibitory range of non-host volatiles in reducing pheromone attraction in European spruce bark beetle *Ips typographus*. *Oikos.* 101:299-310.

814 **Figure Legends**

815

816 **Figure 1. Maximum likelihood phylogeny of odorant receptors (ORs) from beetles of**
817 **Curculionidae and Cerambycidae.** Included are OR amino acid sequences from the
818 curculionids *Hylobius abietis* ('Habi'; red), *Ips typographus* ('Ityp'; blue), *Dendroctonus*
819 *ponderosae* ('Dpon'; orange), and the cerambycid *Megacyllene caryae* ('Mcar'; black). The
820 tree is based on a MAFFT alignment, constructed using FastTree, and rooted with the
821 conserved Orco lineage. The major coleopteran OR groups are indicated by the black arcs
822 (Mitchell, et al. 2020). The twelve groups of simple (1:1:1) OR orthologues across the three
823 curculionids are highlighted in yellow; two clades housing putative simple orthologues shared
824 by the cerambycid *M. caryae* and two of the curculionids are highlighted in purple. Receptors
825 in OR group 2B that were functionally characterized in the present study and the previously
826 characterized McarOR5 (Mitchell, et al. 2012) are labeled by the compounds that activate
827 them (GLV-OHs = green leaf volatile alcohols; 2-PE = 2-phenylethanol). Local node support
828 values were calculated using the Shimodaira-Hasegawa (SH) test implemented in FastTree,
829 and are indicated on branch nodes by the shaded circles; support increases with the brightness
830 of the circles. The sources of sequence data and explanation of receptor suffixes are detailed
831 in the Materials and Methods section.

832

833 **Figure 2. Conserved responses to green leaf volatile (GLV) alcohols in curculionid**
834 **odorant receptor (OR) orthologues. (A)** Response of *Hylobius abietis* OR4 (*Homo sapiens*
835 codon optimized; HabiOR4^{HsCO}) to select compounds in the screening experiments (30 µM
836 stimulus concentration; n = 3 biological replicates, n_{total} = 9). **(B)** Dose-dependent response of
837 HabiOR4^{HsCO} to the five active GLVs, indicating similar sensitivities to four of the
838 compounds (see main text for EC_{50} values; n = 3-5 biological replicates, n_{total} = 9-15). **(C)**
839 Screening responses of *Dendroctonus ponderosae* OR9 (*H. sapiens* codon optimized;
840 DponOR9^{HsCO}; n = 3 biological replicates, n_{total} = 9), and **(D)** dose-dependent responses of
841 DponOR9^{HsCO} to the two most active ligands (n = 5 biological replicates, n_{total} = 15). **(E)**
842 Screening response of *Ips typographus* OR5 (ItypOR5; n = 3-5 biological replicates, n_{total} = 9-
843 15), and **(F)** dose-dependent response of ItypOR5 to the most active ligand (n = 6 biological
844 replicates, n_{total} = 18). Ligand-induced activation was recorded from cells induced (+) to
845 express the exogenous Orco and OR genes and from non-induced (–) control cells. VUAA1
846 was tested at 50 µM as a control for functional Orco expression. Asterisks indicate
847 significantly stronger responses in induced compared to non-induced cells (at $p < 0.001$; see

848 main text for details on statistics). Ligands eliciting < 3% increased fluorescence in screening
849 assays were excluded from dose-response trials. Error bars show SEM. All data from induced
850 and non-induced cells to all 62 test compounds are reported in Supplementary Data 1.
851
852 **Figure 3. Conserved responses to 2-phenylethanol in curculionid odorant receptor (OR)**
853 **orthologues. (A)** Response of *Hylobius abietis* OR3 (HabiOR3) to select compounds in the
854 screening experiments (30 µM stimulus concentration; n = 3-4 biological replicates, n_{total} = 9-
855 12). **(B)** Dose-dependent responses of HabiOR3 (n = 3 biological replicates, n_{total} = 9; see
856 main text for EC_{50} value). **(C)** Screening responses of *Dendroctonus ponderosae* OR8 (*H.*
857 *sapiens* codon optimized; $DponOR8^{HsCO}$; n = 3 biological replicates, n_{total} = 9), and **(D)** dose-
858 dependent responses of $DponOR8^{HsCO}$ (n = 9 biological replicates, n_{total} = 27; see main text
859 for EC_{50} value). **(E)** Screening responses of *Ips typographus* OR6 (ItypOR6; n = 3 biological
860 replicates, n_{total} = 9), and **(F)** dose-dependent responses of ItypOR6 (n = 3 biological
861 replicates, n_{total} = 9; see main text for EC_{50} value). Ligand-induced activation was recorded
862 from cells induced (+) to express the exogenous beetle Orco and OR genes and from non-
863 induced (–) control cells. VUAA1 was tested at 50 µM as a control for functional Orco
864 expression. Asterisks indicate significantly stronger responses in induced compared to non-
865 induced cells (at $p < 0.001$; see main text for details on statistics). Error bars show SEM. All
866 data from induced and non-induced cells to all 62 test compounds are reported in
867 Supplementary Data 1.

Figure 1.

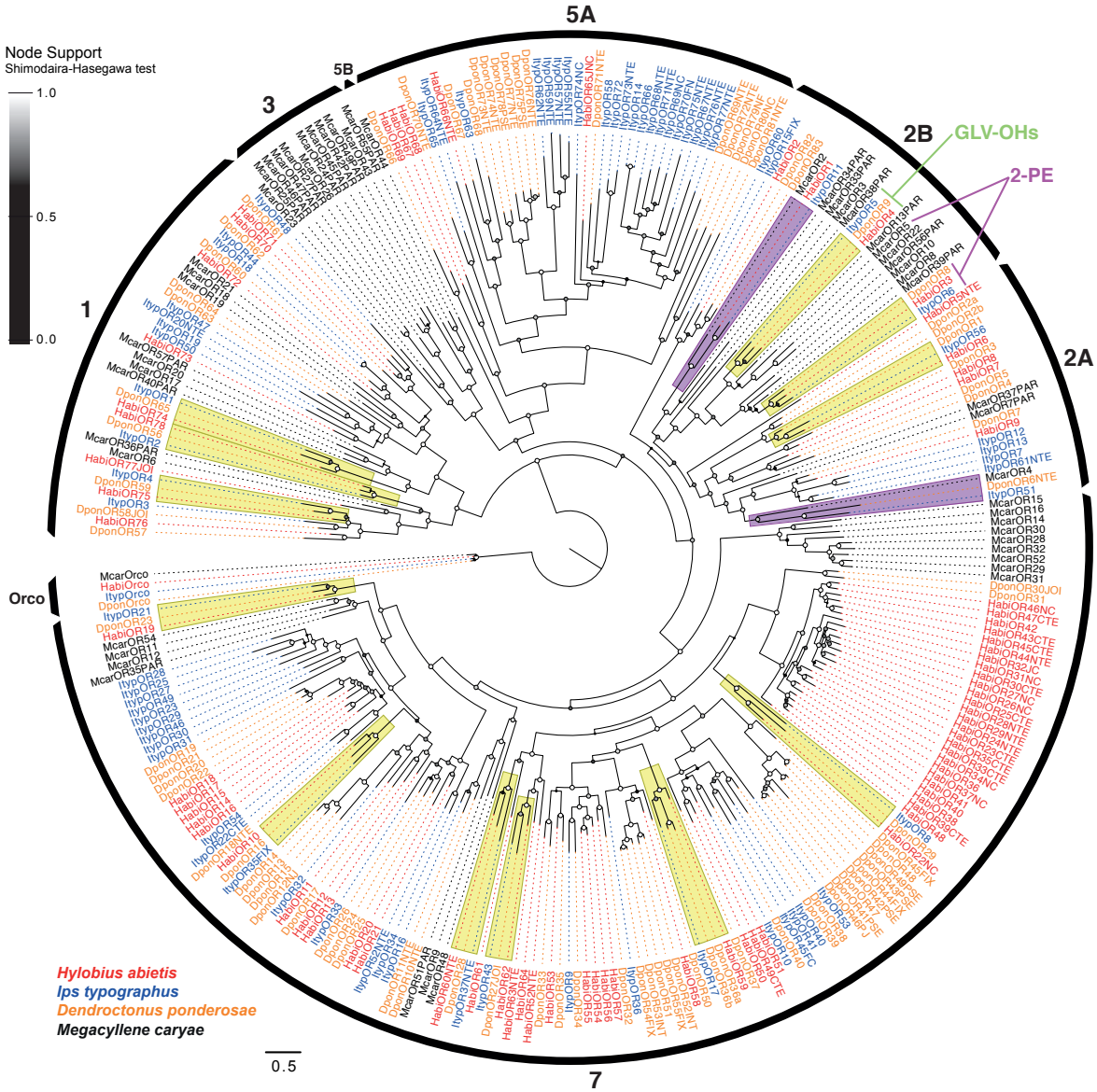
Node Support
Shimodaira-Hasegawa test
1.0
0.5
0.0
5A
5B
3
1
2B
2A
7
Orco
GLV-OHs
2-PE
Hylobius abietis
Ips typographus
Dendroctonus ponderosae
Megacyllene caryae
0.5

871 **Figure 2.**

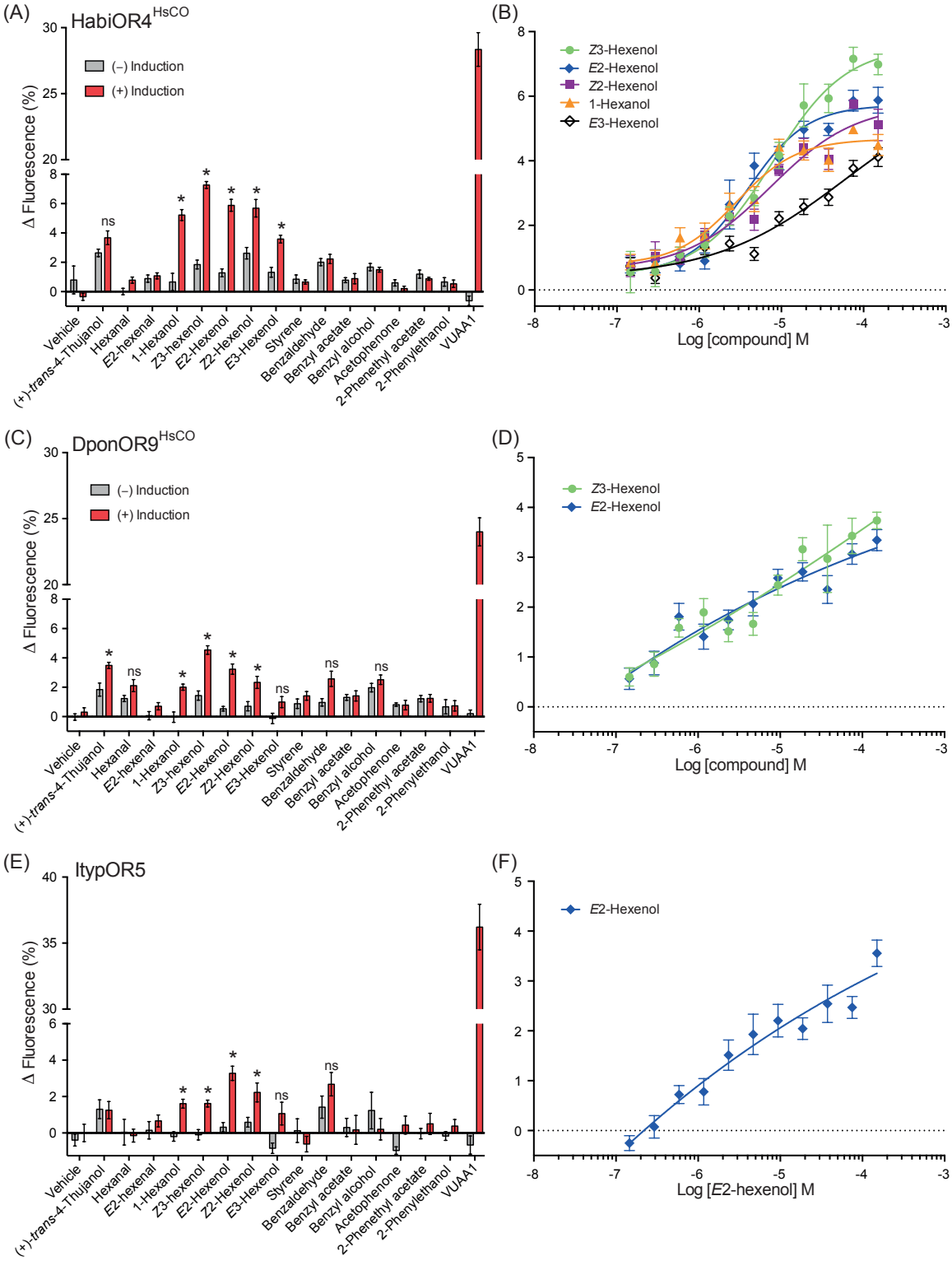

872

873

874 **Figure 3.**

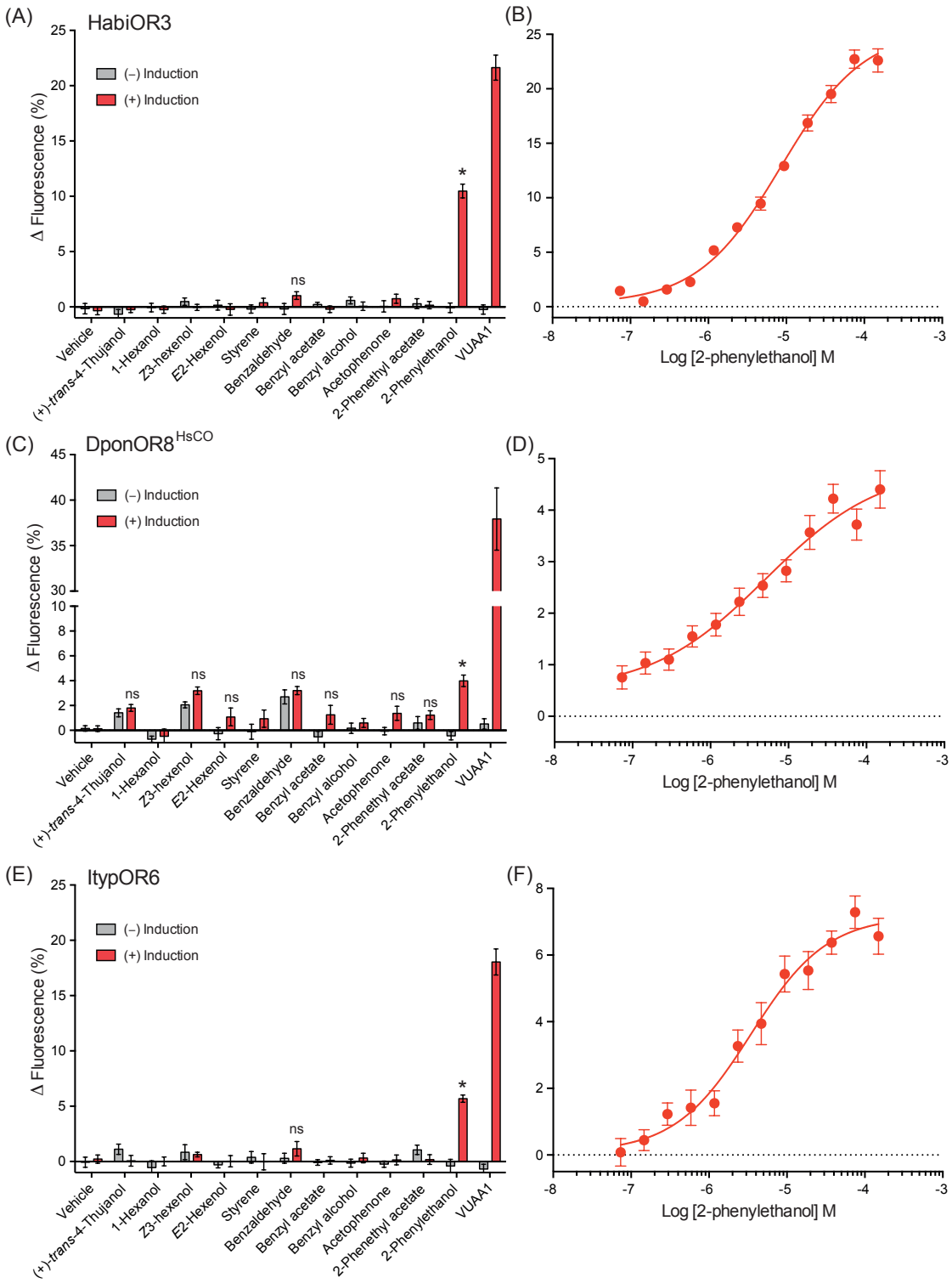

875